

Microscale distribution of zooplankton in relation to turbulent diffusion

Marie Maar

National Environmental Research Institute, Department of Marine Ecology, Frederiksborgvej 399, DK-4000 Roskilde; and Department of Marine Ecology, University of Aarhus, Finlandsgade 14, DK-8200 Århus, Denmark

Torkel Gissel Nielsen

National Environmental Research Institute, Department of Marine Ecology, Frederiksborgvej 399, DK-4000 Roskilde, Denmark

Adolf Stips

Inland and Marine Waters Unit, CEC Joint Research Centre, TP 272, I-21020 Ispra, Italy

André W. Visser

Department of Marine Ecology and Aquaculture, Danish Institute for Fisheries Research, Kavalergaarden 6, DK-2920 Charlottenlund, Denmark

Abstract

Microscale vertical distribution of proto- and mesozooplankton in relation to turbulent diffusion was investigated using a high-resolution sampler (HSR) during cruises in the Skagerrak, Denmark, and the Northern Aegean, Greece. A strong pycnocline and a deep chlorophyll maximum (DCM) characterized both areas. The phytoplankton biomass in the Skagerrak was much higher and dominated by netplankton compared with the Aegean, where picoplankton dominated. Deployments of the HRS and measurements of microscale turbulence were made simultaneously in the mixed surface layer, the pycnocline, and the DCM and revealed a large range (0.2–250 cm² s⁻¹) in turbulent diffusion. In general, turbulent diffusion was highest in the surface layer. The variability of the plankton organisms within the 3-m strata sampled by the HRS was quantified by their coefficient of variation (CV = SD/mean) and analyzed with respect to turbulent diffusion. We hypothesized that the variability of the vertical distribution would be independent of turbulence up to a threshold where dispersion overwhelms the swimming ability of the organism and variability decreases. The hypothesis was confirmed by our results; for the weak swimmers, ciliates, *Ceratium* spp., and nauplii, there was a significant decrease in CV with increasing turbulence, whereas the variability of the stronger swimmer represented by copepodites was uncorrelated with turbulent diffusion. This underscores the potential of these organisms in locating and exploiting food patches in the water column.

Plankton are, per definition, passive drifters in the water. However, zooplankton are not homogeneously distributed in the water column but occur in patches. The two main mechanisms behind this discrepancy are zooplankton swimming behavior and the physical-chemical properties of the environment.

Zooplankton can adjust their vertical position in the water column by swimming or sinking. Aggregations of herbivorous zooplankters often coincide with prey patches, for ex-

ample, in subsurface chlorophyll *a* peaks (Ortner et al. 1980; Richardson et al. 1998) or in local patches of aggregates or protozooplankton (Mackas et al. 1993). In environments where the average food concentration is limiting for zooplankton growth, encounters with food patches are essential for the survival success and growth of zooplankton. Both modeling (Tiselius et al. 1993; Leising and Franks 2000) and experimental work (Tiselius 1992; Saiz et al. 1993; Fenchel and Blackburn 1999) have shown that copepods and protozoans can detect and exploit such patches and thus increase their survival success.

Turbulence influences the encounter rate between predators and prey. In a model by Davis et al. (1991), intermediate turbulence levels disperse prey patches and zooplankton growth decreases in comparison with low turbulence conditions. However, at higher turbulence, the encounter rate between predator/prey increases and the zooplankton growth rate is restored to original values. At very high levels of turbulence, the copepods are stressed and growth rates are reduced (Saiz and Kiørboe 1995). Variable profiles of turbulence will influence the vertical distribution of zooplankton. It has been observed that copepods respond to changes in the local intensity of turbulent mixing by altering their

Acknowledgments

We thank the crews of the RVs *Dana* and *Aegeo* and Peter Tiselius, Kajsa Tönnesson, Tanya Zervoudaki, and Epaminondas D. Christou for assistance during the cruises. The high quality of turbulence data was achieved because of the numerous efforts taken by Hartmut Prandke in doing the turbulence measurements and careful data analysis and processing done by Ute Tschesche. We acknowledge Saskia Gooding for counting the Skagerrak samples, Lars Gissel Nielsen for designing the HRS, and Katherine Richardson for valuable comments. Two anonymous reviewers are acknowledged for their detailed and constructive comments to an earlier version of our manuscript. The project was financially supported by a KEYCOP grant (MAST III: MAS3-CT97-0148) and a Danish National Research Council grant (9801391).

depth preference, avoiding the most turbulent parts of the water column (Mackas et al. 1993; Visser et al. 2001).

The ability of zooplankton to aggregate in prey patches, to avoid regions of high turbulent mixing or predators, depends on their swimming strength with respect to local turbulent diffusion. Zooplankton organisms with a low swimming potential will have difficulty in overcoming turbulent diffusion and eventually will be dispersed. In a field study, it was observed that wind-induced mixing redistributed copepod nauplii, whereas the copepodites were less influenced (Andersen et al. 2001). Other field studies have also documented a greater patchiness of organisms with increasing swimming speed (Owen 1989; Tiselius et al. 1994; Olli 1999).

Conventional water bottles integrates over intervals of 0.5–1 m in the water column—that is, the scale of sampling is much greater than the small-scale variance of zooplankton and concentrations determined from such samples are average estimates over these depths. To fully understand the distribution patterns of zooplankton, it is necessary to study the interactions between different organisms and the environment on the same scale as for the organisms. Microscale patchiness (centimeters to meters) of zooplankton has so far received little attention.

In the present study, we deployed a vertical high-resolution sampler (HRS) together with a microstructure shear (MSS) profiler in the Skagerrak (Denmark) and the northern Aegean Sea (Greece) (Fig. 1). The Skagerrak is a mesotrophic system influenced by the outflow of brackish water from the Baltic Sea and the inflow of high-salinity water from the North Sea. The surface currents form a large cyclonic circulation and are associated with a dome-shaped pycnocline in the system (Rohde 1998). The northern Aegean Sea is a subsystem of the oligotrophic eastern Mediterranean, and the inflow of brackish water from the Black Sea creates a front in the area (Stergiou et al. 1997). Both areas are stratified by a halocline most of the year, and food is potentially limiting for copepod growth during the summer period (Kjørboe and Nielsen 1994; Stergiou et al. 1997).

The aim of the present study was to investigate microscale variability in distributions of different plankton organisms with respect to turbulent diffusion. The vertical microscale variability (patchiness) was estimated as the coefficient of variation of 20 samples over a 3-m depth strata. We hypothesized that the vertical microscale distribution of zooplankton with a specific swimming ability would be independent of turbulent diffusion up to a certain turbulence threshold after which variability would decrease with increasing turbulent diffusion.

Materials and methods

HRS—To study vertical microscale patchiness of zooplankton organisms, a vertical HRS was deployed in the Skagerrak, Denmark, and the northern Aegean Sea, Greece (Fig. 1). On the basis of the conductivity-temperature-depth (CTD) and fluorescence profiles, one or two depth strata were selected for sampling with the HRS at the different stations (Table 1).

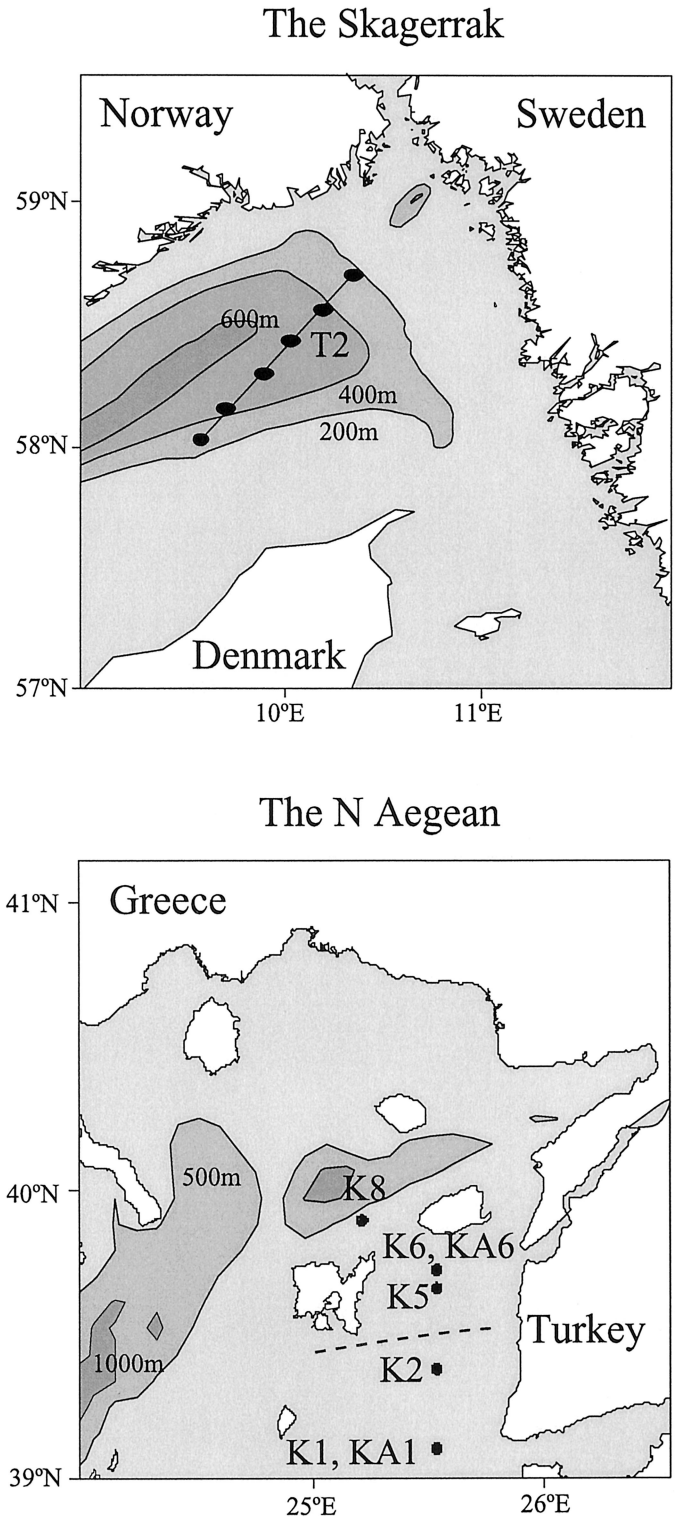


Fig. 1. Map of the Skagerrak and the northern Aegean with the sampling stations. In the northern Aegean, Sta. K5, K6/A6, and K8 were located in the front, whereas Sta. K1/A1 and K2 were located outside the frontal area indicated with a dotted line.

Table 1. The sampled stations with depth, date, location, water column layer (surface mixed layer, deep Chl *a* maximum (DCM), and pycnocline), dissipation rate (ε), and turbulent diffusion (K) in the north Aegean and the Skagerrak.

Location	Sta.	Depth (m)	Date	Latitude N	Longitude E	Layer	ε (10^{-4} cm ² s ⁻³)	K (cm ² s ⁻¹)
The N Aegean 1999	K1	10	23 Sep 1999	39°25'72"	25°43'78"	Mixed	30	250
	K2	10	24 Sep 1999	39°39'82"	25°44'95"	Mixed	10	9.5
	K2	64	24 Sep 1999	39°39'82"	25°44'95"	DCM	6	4.3
	K5	5	26 Sep 1999	39°54'19"	25°44'99"	Mixed	20	3.6
	K5	55	26 Sep 1999	39°54'19"	25°44'99"	DCM	6	1.1
	K6	5	28 Sep 1999	39°58'55"	25°44'99"	Mixed	40	1.2
	K6	25	28 Sep 1999	39°58'55"	25°44'99"	Pycnocline	10	0.2
	K8	28	29 Sep 1999	40°08'24"	25°22'28"	Pycnocline	8	0.7
The N Aegean 2000	K8	44	29 Sep 1999	40°08'24"	25°22'28"	DCM	8	0.8
	KA1	12	02 Apr 2000	39°27'71"	25°44'70"	Mixed	20	20
	KA1	33	02 Apr 2000	39°27'71"	25°44'70"	Pycnocline	5	7.0
	KA6	12	06 Apr 2000	39°57'72"	25°44'93"	Mixed	40	120
The Skagerrak 2000	KA6	23	06 Apr 2000	39°57'72"	25°44'93"	Pycnocline	3	0.7
	T2	12	28 Aug 2000	58°26'14"	10°02'87"	Pycnocline	400	4.8
	T2	23	28 Aug 2000	58°26'14"	10°02'87"	DCM	4	7.9

The sampler is composed of 20 pairs of 1.5-liter polycarbonate syringes (Linatex) mounted in pairs on each side of a 300 × 100 cm metal frame (Fig. 2). The distance between each syringe is 15 cm. A silicone valve protects the entrance of each syringe. The plungers of each pair of syringes are mounted on a central wire. The central wire is connected to the release system in the top of the sampler. The release system consists of a Volvo spring. When loaded, the syringes are empty and the spring is compressed and kept in position by a trigger. Dropping a messenger along the wire releases the trigger. As the spring expands, the central wire moves 30 cm and the syringes are immediately filled. Water from the duplicate bottles at each depth was pooled to achieve a sufficient sampling volume for estimating zooplankton abundance. The position of the sampler was determined by a pressure sensor in a Dr. Haardt fluorometer mounted in the middle of the frame. To minimize vertical mixing by the HRS, the opening of the syringes were kept facing into the current by three large fins mounted on the backside of the metal frame.

The Skagerrak—The HRS was deployed twice at Sta. T2 in August 2000 (Table 1) from the RV *Dana* (Danish Institute for Fisheries Research). Profiles of temperature, salinity, and fluorescence were measured from the surface to 100 m depth using a CTD system (911+) equipped with a Dr. Haardt fluorometer. In situ fluorescence measurements were calibrated against Chl *a* concentrations evaluated at seven depths at Sta. T2 from 5-liter Niskin bottles ($r^2 = 0.95$, $P < 0.05$). Water samples of 500 ml were filtered onto GF/F filters, extracted in 5 ml 96% ethanol for 6–24 h, and measured before and after addition of acid on a Turner Designs Model 700 Fluorometer (Yentsch and Menzel 1963).

The Aegean Sea—There were nine deployments with the HRS during the September cruise (1999) and four deployments during the April cruise (2000) (Table 1) aboard the RV *Aegeo* (National Center of Marine Research). Profiles of temperature, salinity, and fluorescence were measured from

the surface to 100 m depth using a Seabird CTD system (911+) equipped with a fluorometer. In situ fluorescence measurements were calibrated against Chl *a* concentrations evaluated at eight depths at Sta. K6 from 10-liter Niskin bottles ($r^2 = 0.96$, $P < 0.05$). For analysis, see above.

Turbulence—Microstructure velocity shear was measured with a MSS profiler (serial number 007) from the Joint Research Centre (Prandke and Stips 1998). The profiler was equipped with two velocity microstructure shear sensors (type PNS98), a microstructure temperature sensor, and three standard CTD sensors, as well as a sensor to measure horizontal acceleration of the profiler (Prandke et al. 2000). The profiler was balanced to have negative buoyancy in the water column, which gave it a sinking velocity of ~ 0.7 -m s⁻¹. The data were sampled at a frequency of 1,024 Hz. The shear sensors were calibrated before and after the campaigns and the sensitivity was checked daily during the campaigns using the shear sensor test device TSS. This allowed us to account for changes in the sensitivity of the sensors. From these measurements we computed the dissipation rate of the turbulent kinetic energy and the Brunt-Väisälä frequency (buoyancy frequency) squared (for details, see Prandke et al. 2000) over depth intervals of 0.5-m length. The computing procedure included the removal of spiky data, as well as the removal of low-frequency disturbances and high-frequency noise using specially constructed filters. The shear data were first differenced, and the power spectrum was calculated in the observed wavenumber range. Then an iterative procedure was applied to determine the Kolmogorov wavenumber, which represents the upper bound for integrating the shear spectrum. Under the assumption of isotropy at the smallest scales, the viscous dissipation rate is calculated for each sensor separately, using only one component of the shear tensor. Finally, the dissipation rate was corrected for the lost variance below and above the integration limits used, under the assumption of a universal form of the shear spectrum.

The uncertainties in estimating the turbulent dissipation rate ε have been discussed by Oakey (1982), Moum and

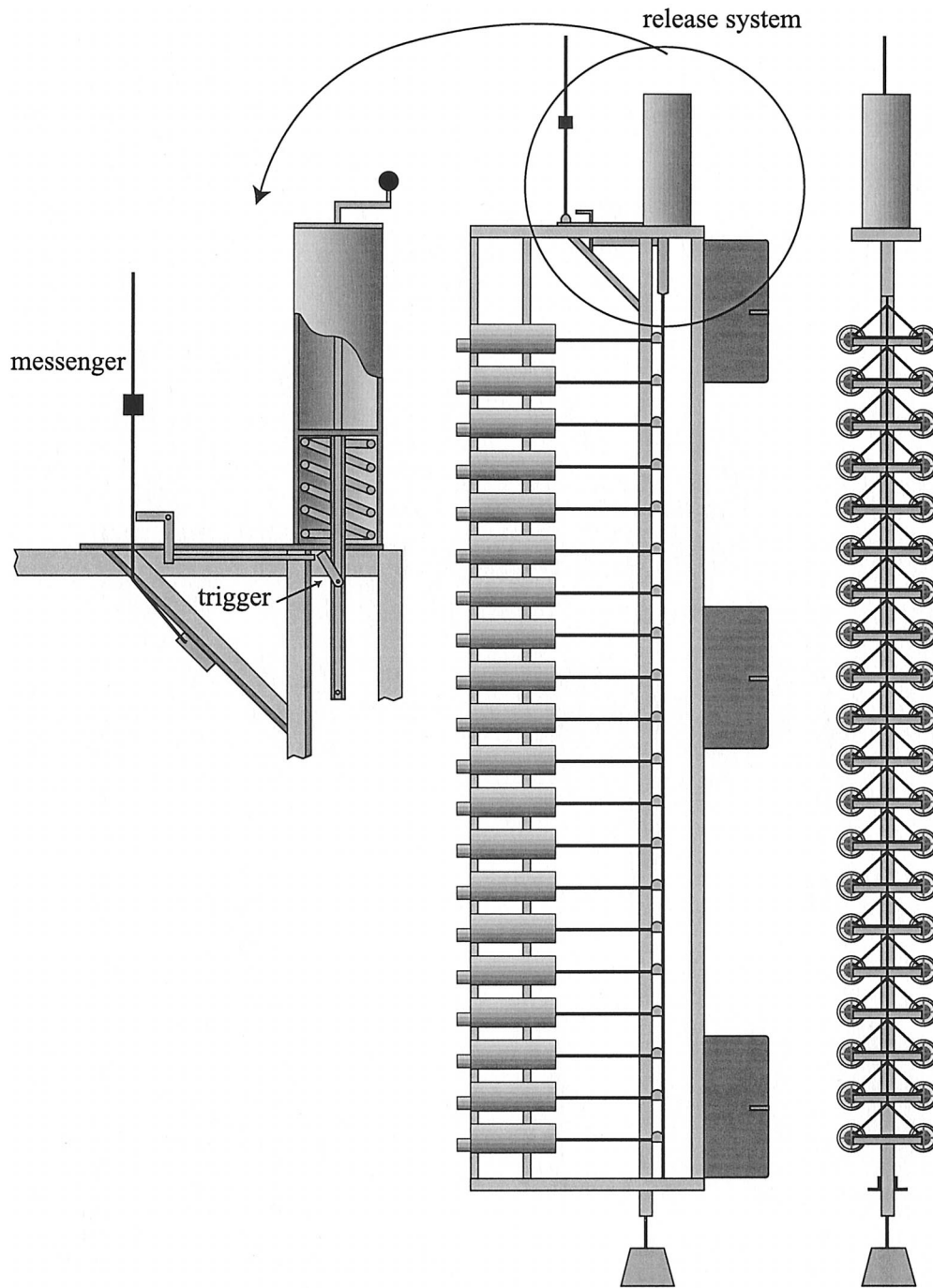


Fig. 2. The HRS. See text for explanations.

Lueck (1985), and Peters et al. (1988), and we will only briefly discuss certain aspects not covered in those papers. With respect to the present work, the overriding interest is not so much the absolute accuracy in measuring ε but the precision or consistency of the measurements in itself (relative error).

The most critical problem is the determination of the flow rate past the sensor, because ε depends on its fourth power. We estimate the flow rate as the fall speed of the profiler.

This will be only correct if the vertical velocity of the water is zero and the profiler falls with no tilt angle. Using a typical fall speed of $\sim 0.7 \text{ m s}^{-1}$ the uncertainty in the flow rate will be $\sim 1\%$ and thus could contribute 4%–5% to the uncertainty in ε .

The calibration uncertainty leads to an inaccuracy in the sensitivity of a probe and would cause a systematic uncertainty in the estimated ε values from that probe. Investigations by Prandke et al. (2000) have proved that these uncer-

tainties are in the order of 10%. Such an inaccurate overall ε estimate has no influence on the conclusions drawn in the present article.

More critical, but rarely discussed in the published literature, is the loss of sensitivity of many shear probes when they are immersed in water and subject to pressure. This loss of sensitivity is caused by the penetration of water molecules into the isolation and a subsequent reduction in the isolation resistance of the piezoceramic bending element. It depends on the type of shear sensor used but also differs for shear probes of the same type. The calibration typically applied before and after a cruise will not reveal this sensitivity loss, because the sensors, when out of water will dry and regain their original sensitivity within a few days (Prandke et al. 2000). To cope with this problem, we checked the calibration daily onboard using the shear sensor test device TSS to determine time varying sensitivity during the cruise (Stips et al. 2001). Of the two sensors mounted at the probe, one had a constant sensitivity, whereas the second lost 15% of its sensitivity during the first 3 days of the Skagerrak cruise and remained constant thereafter. This was used to improve estimates of ε .

Another source of uncertainty is the variance-loss correction scheme that corrects individual spectra for incomplete resolution of the turbulence spectra. We used the simplified method given in Prandke et al. (2000) systematically for all the campaigns.

A further methodological uncertainty results from the application of the isotropic formulation using only one shear tensor component. This was checked by mounting the two shear probes perpendicular to each other so that they measured two independent shear components. Both produced ε estimates that agreed within 20% and were well correlated. Thus, we can conclude that application of the isotropic formula is reasonable, and any related error is limited to $\sim 20\%$.

A more general methodological problem is our limited ability of resolving the real space-time variability of the turbulence field by discrete vertical profiles. This becomes especially critical during multidisciplinary investigations, where the wire time attributed to each group is limited. Bursts of three consecutive turbulence profiles were taken before and after each biological sampling and were averaged over the vertical length of the biological sampling or 5-m depth intervals, respectively. Despite ongoing discussions as to the appropriate averaging procedure for turbulent quantities, we followed Davies (1996) in presenting direct arithmetic averages of the measured dissipation rate. About 60–100 ε estimates are represented as a single point in the mean profiles (Fig. 3), and the variance is sufficiently small ($\sim 20\%$) that larger vertical differences can be safely discussed.

Moum et al. (1995) made an interplatform comparison of ε measurements and concluded that an estimate of the uncertainty in the mean values of 100% is perhaps a conservative estimate. From previous discussions, we basically agree on this but think that the relevant relative error here will more likely be $< 50\%$. Because, when calculating turbulent diffusivity with mixing efficiency, a new uncertainty enters, we apply the 50% error estimate to the respective

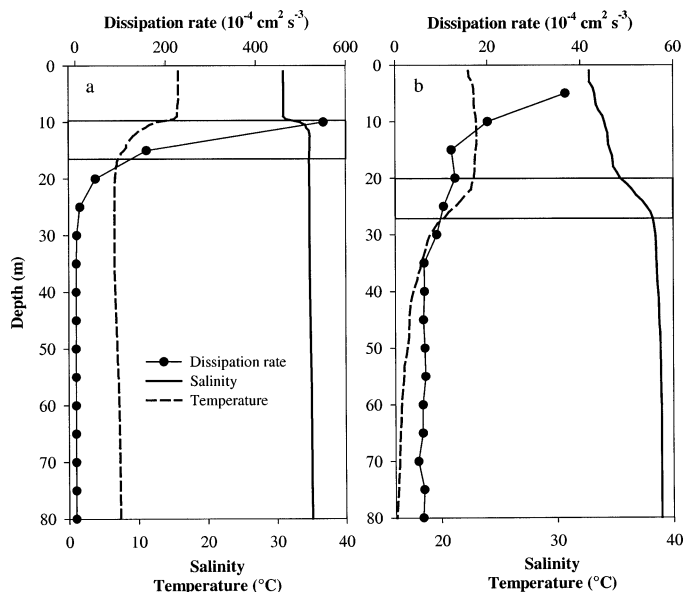


Fig. 3. Vertical profiles of salinity, temperature, and dissipation rate at (a) Sta. T2, the Skagerrak, and (b) Sta. K6, the northern Aegean.

correlation plots, keeping in mind that the accuracy might be less.

The depth where dissipation measurements can be considered reliable during falling measurements depends on the drift speed and the draft of the vessel. In situations without wind and drift, we consider that measurements are reliable below 5 m depth (see Fig. 3b, Sta. K6), whereas with wind and strong drift, reliable measurements are only available from 10 m down (see Fig. 3a, Sta. T2).

Turbulent eddy diffusivity is herein referred to as “turbulent diffusivity” and is a measure of the efficiency of the turbulent eddies to disperse particles. Turbulent eddy diffusivity (K) within a stratified fluid was estimated from (Osborn 1980):

$$K = e\varepsilon/N^2 \quad (1)$$

where e is a mixing efficiency ($e = 0.2$ herein), ε is the turbulent dissipation rate, and N is the Brunt-Väisälä frequency.

Chl a—Chl *a* was determined from 100-ml water samples filtered onto GF/F filters, extracted in 5 ml 96% ethanol for 6–24 h, and measured before and after addition of acid on a Turner Designs Model 700 Fluorometer (Yentsch and Menzel 1963).

Lugol samples—Samples for analysis of compositions of protozooplankton were preserved with acidified Lugol’s solution (2% final concentration). Subsamples of 10 ml from the Skagerrak were settled for 24 h prior to enumeration and identification at $200\times$ magnification (Nielsen and Hansen 1999). Diatoms and nanoflagellates ($2\text{--}20\ \mu\text{m}$) were also counted in a sample from 10 and 25 m at $400\times$ magnification. The cell volumes were converted to carbon according to the method of Menden-Deuer and Lessard (2000).

Table 2. The mean (\pm SD) Chl *a* values and the mean (\pm SD) concentration of organisms in Lugol samples (100 ml) and in formol samples indicated with the mean filtered volume (\pm SD). *, counted in 10 ml lugol samples from the Skagerrak, and —, data discarded because of too few mean counts per sample. The depth is indicated with water column layer: M, mixed; D, DCM; and P, pycnocline.

Sta.	Depth (m)	Layer	Chl <i>a</i> ($\mu\text{g L}^{-1}$)	Ciliates (cell L^{-1})	Mean vol. (L)	<i>Ceratium</i> spp. (cells L^{-1})	Nauplii (ind. L^{-1})	Copepodites (ind. L^{-1})
K1	10	M	0.06 \pm 0.01	49 \pm 13	1.28 \pm 0.15	—	4.2 \pm 1.0	3.9 \pm 2.3
K2	10	M	0.18 \pm 0.01	57 \pm 16	1.24 \pm 0.19	—	7.7 \pm 2.0	—
K2	64	D	0.47 \pm 0.05	—	1.24 \pm 0.17	—	6.7 \pm 2.7	3.9 \pm 2.2
K5	5	M	0.35 \pm 0.02	450 \pm 130	1.42 \pm 0.20	52 \pm 16	10 \pm 3.8	8.3 \pm 2.6
K5	55	D	0.52 \pm 0.02	200 \pm 73	1.47 \pm 0.23	6.4 \pm 3.6	8.8 \pm 3.5	3.6 \pm 1.8
K6	5	M	0.27 \pm 0.01	280 \pm 100	1.29 \pm 0.18	44 \pm 16	16 \pm 4.4	8.7 \pm 3.2
K6	25	P	0.33 \pm 0.02	170 \pm 80	1.42 \pm 0.23	—	9.7 \pm 3.4	—
K8	28	P	0.28 \pm 0.02	230 \pm 100	1.46 \pm 0.21	10 \pm 4	10 \pm 3.7	—
K8	44	D	0.35 \pm 0.04	150 \pm 62	1.48 \pm 0.22	5.0 \pm 3.1	5.8 \pm 1.9	—
KA1	12	M	0.26 \pm 0.02	No data	1.01 \pm 0.15	13 \pm 4	8.8 \pm 3.1	5.7 \pm 2.7
KA1	33	P	0.38 \pm 0.04	No data	0.97 \pm 0.17	19 \pm 5	9.0 \pm 2.9	5.4 \pm 2.9
KA6	12	M	0.29 \pm 0.02	No data	0.81 \pm 0.14	44 \pm 11	18 \pm 4.2	8.0 \pm 4.4
KA6	23	P	0.23 \pm 0.02	No data	0.88 \pm 0.15	43 \pm 14	9.7 \pm 4.5	5.8 \pm 2.8
T2	12	P	3.0 \pm 0.3	1,800 \pm 600*	0.88 \pm 0.11	560 \pm 230*	71 \pm 21	10 \pm 5.0
T2	23	D	11 \pm 1.2	1,900 \pm 410*	0.93 \pm 0.16	2,100 \pm 650*	31 \pm 8.4	6.0 \pm 3.0

Subsamples of 100 ml from the Aegean Sea were allowed to settle for a week in brown 100-ml glass bottles from which 85-ml of the supernatant was later gently siphoned off. The remaining 15 ml was transferred to a centrifuge glass and allowed to settle for 2 d. The upper 13 ml was again siphoned off, and the final 2 ml was mixed and transferred to tissue culture trays (Nunc Multi wells) of 24 wells with a diameter of 18 mm. Aloricate ciliates $>20 \mu\text{m}$ were counted in the whole chamber using an inverted microscope at 200 \times magnification. Other groups of protozooplankton were ignored because of low abundance.

Formol samples—For enumeration of copepodites, nauplii, and *Ceratium* spp., a mean sample volume of 0.81–1.48 liter (Table 2) from the HRS were filtered onto a 21- μm sieve and fixed in 2% buffered formol (final concentration). The coefficient of variation (CV = SD/mean) of the filtered volume was 12%–17% within each cast. The organisms were identified and counted using a light microscope (Olympus) at 40 \times magnification.

Statistical analysis—The zooplankton selected for analysis needed a mean abundance of at least five cells or individuals per sample within a HRS profile (20 replicates) to stabilize the CV (Mouritsen and Richardson unpubl. data). To achieve sufficient counts, the following groups were pooled: (1) all copepodite stages of the cyclopid and cal-

anoid species in the size range 125–750 μm , (2) all nauplii stages and species, (3) all *Ceratium* species, and (4) all aloricate ciliates $>20 \mu\text{m}$. After this data reduction, the vertical microscale variability for each HRS profile was estimated as the CV multiplied by 100%. For regression analyses, the least-squares model with a type I error of 0.05 was used. For the Mann-Whitney *U* test, a type I error of 0.10 was used. All statistical tests were conducted using the Statistical Package of Social Science (SPSS version 10.0) for Windows.

Results

Hydrography—The term “pycnocline” herein refers to the primary pycnocline—that is, the steepest density gradient in the water column. At Sta. T2 in the Skagerrak, the pycnocline was located at 9–15 m depth, and a deep Chl maximum (DCM) was present at 20–30 m depth (Figs. 3a, 4a). In the northern Aegean, the pycnocline was located at 20–35 m depth, and the DCM was located deeper in the water column (40–65 m) than in the Skagerrak (Figs. 3b, 4b, Table 1). Sta. K5, K6/KA6, and K8 were located inside the front, whereas Sta. K1/KA1 and K2 were located outside the brackish plume from the Black Sea (Fig. 1). Sea surface temperatures were 15–16 $^{\circ}\text{C}$ in the Skagerrak and 20–22 $^{\circ}\text{C}$ in September and 12–15 $^{\circ}\text{C}$ in April in the northern Aegean.

The wind conditions were calm during deployments of the HRS, and the surface turbulent dissipation rate was low

Table 3. Mean (\pm SD) abundances and CV values of dinoflagellates in the Skagerrak.

Taxon	Pycnocline		DCM	
	Mean \pm SD	CV	Mean \pm SD	CV
<i>Ceratium furca</i>	16,000 \pm 2,800	18	10,000 \pm 2,600	26
<i>Prorocentrum micans</i>	500 \pm 230	46	910 \pm 36	40
<i>Dinophysis norvegica</i>	800 \pm 390	49	760 \pm 440	58
<i>Dinophysis</i> spp.	1,200 \pm 300	25	2,600 \pm 800	31
<i>Gyrodinium spirale</i>	370 \pm 440	120	1,300 \pm 1,400	110

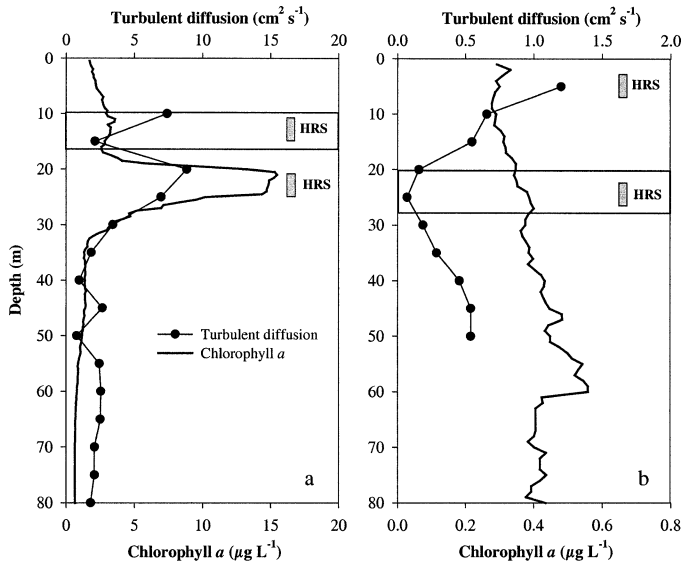


Fig. 4. Vertical profiles Chl *a* and turbulent diffusion and the positions of the pycnocline and the HRS at (a) Sta. T2, the Skagerrak, and (b) Sta. K6, the northern Aegean.

(<0.06 cm² s⁻³). The dissipation rate decreased drastically with depth, and the measured values were in the range of 3–400 × 10⁻⁴ cm² s⁻³ (Table 1). At Sta. T2, the high dissipation rate at the pycnocline was caused by a velocity shear between the surface layer and the pycnocline and not by wind stress as for the Aegean stations.

Plankton distributions—In the Skagerrak, the Chl *a* concentration was 3.0 µg L⁻¹ at the pycnocline and 11.0 µg L⁻¹ at the DCM (Table 2). The higher phytoplankton biomass at the DCM was confirmed by microscope examinations, which gave a biomass of 531 µg C L⁻¹ compared with 84 µg C L⁻¹ at the pycnocline. Microscopic inspection also showed that 88% of the biomass at the DCM consisted of diatoms (mainly *Leptocylindrus danicus*), whereas *Ceratium* spp. and “other” flagellates (*Dinophysis* spp., *Prorocentrum* spp., cryptophytes, and prasinophytes) constituted 8% and 4%, respectively. At the pycnocline, 76%, 19%, and 5% of the biomass was *Ceratium* spp., “other” flagellates (see above), and diatoms, respectively. *Ceratium furca* occurred in very high numbers with little variability in abundance compared with the other taxon groups (Table 2, 3) and has therefore been omitted from the analysis of variability.

Ciliates had similar abundances at both depth strata (Table 2), whereas *Gyrodinium spirale* was most abundant at the DCM (Table 3). The biomass of ciliates and heterotrophic dinoflagellates was 3.2 ± 0.7 µg C L⁻¹ at the pycnocline and 26.7 ± 3.6 µg C L⁻¹ at the DCM.

In the Aegean, the much lower Chl *a* concentrations (0.06–0.52 µg L⁻¹) (Table 2) increased with depth (Fig. 5). Inside the frontal area, there was a higher primary production and a higher abundance of small dinoflagellates, small diatoms (Pagou et al. pers. comm.), *Ceratium* spp., and ciliates (Table 2) at the surface layer than at the DCM. The picoplankton (0.2–1.2 µm) consisting of cyanobacteria were, nevertheless, the most important contributor to phytoplank-

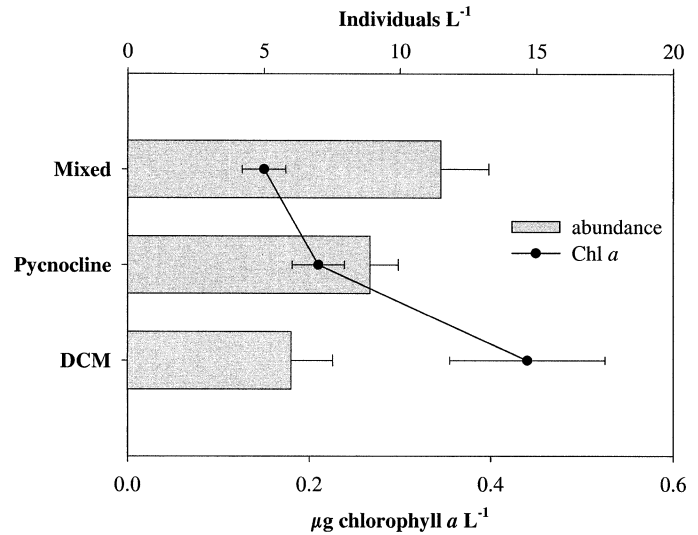


Fig. 5. The mean (±SE) copepodite and nauplii abundance and Chl *a* at the mixed, pycnocline, and DCM layers in the frontal area of the northern Aegean.

ton biomass and primary production at all stations (Pagou et al. pers. comm.).

The abundance of nauplii was also higher in the Skagerrak than in the Aegean, whereas the abundance of copepodites (calanoid and cyclopid species) was comparable. Because of the small sampling volume (<1.5 liters), only the smaller, most abundant copepods were caught by the HRS. In the Skagerrak, *Paracalanus* spp. and *Oithona* spp. dominated, while the most abundant species in the Aegean were *Clausocalanus* spp., *Oithona* spp., *Oncaea* spp., and *Corycaeus* spp. The vertical distribution of nauplii and copepodites decreased from the upper mixed layer/pycnocline toward the DCM at Sta. T2 (Table 2) and at the frontal stations in the northern Aegean (Fig. 5). At Sta. K1, KA1, and K2, there was no depth partitioning among nauplii and copepodites.

Microscale patchiness—The HRS was deployed in the mixed surface layer, the pycnocline, or the DCM to achieve the highest range of turbulent diffusion values possible (Table 1). The range of turbulent diffusion values obtained was 0.2–250 cm² s⁻¹. The average turbulent diffusion was significantly higher in the surface mixed layer than in the pycnocline and the DCM (Table 4).

The vertical profiles of Chl *a*, turbulent diffusion, and the positions of HRS sampling are shown for Sta. T2 in the Skagerrak and Sta. K6 in the Aegean (Fig. 4). The turbulent diffusivity was similar in the pycnocline at Sta. T2 and in the mixed layer at Sta. K6 (Table 1). The HRS profiles of Chl *a*, ciliates, *Ceratium* spp., nauplii, and copepodites from these two layers show that, despite the difference in plankton abundances between the two areas, microscale patchiness was comparable at similar turbulent diffusion rates (Fig. 6).

We tested whether the variability (expressed as CV values) of Chl *a* and zooplankton organisms from all stations was different between the layers in the water column (mixed, pycnocline, and DCM) (Table 4). To obtain sufficient replicates (>4), the data from the pycnocline and DCM layers

Table 4. The average turbulent diffusion (\pm SD) and the mean CV (%) of Chl *a*, “ciliates and *Ceratium* spp”, nauplii, and copepodites from the water column layers (*n* = number of replicates). For the given parameters, the significance level of the difference between the surface mixed layer versus the pycnocline and DCM is shown (Mann–Whitney *U*-test, $P < 0.10$).

Layer	Turbulent diffusion (cm ² s ⁻¹)	Mean CV			
		Chl <i>a</i>	Ciliates + <i>Ceratium</i>	Nauplii	Copepodites
Mixed	68 \pm 101 (<i>n</i> =6)	7 (<i>n</i> =6)	30 (<i>n</i> =8)	29 (<i>n</i> =6)	45 (<i>n</i> =5)
Pycnocline	2.7 \pm 3.3 (<i>n</i> =5)	9 (<i>n</i> =5)	42 (<i>n</i> =7)	35 (<i>n</i> =5)	53 (<i>n</i> =3)
DCM	3.5 \pm 3.0 (<i>n</i> =4)	9 (<i>n</i> =4)	39 (<i>n</i> =6)	36 (<i>n</i> =4)	50 (<i>n</i> =3)
Significance level	$P=0.02$	NS	$P=0.03$	$P=0.07$	NS

(with similar turbulent diffusion levels) were pooled. The hypothesis investigated was that the microscale variability of plankton distributions would be lowest in the mixed layer, where the turbulent diffusivity was higher than that found in the pycnocline and DCM. Because the data were not normally distributed, the nonparametric Mann-Whitney *U* test

was used. No significant differences between water-column layers for Chl *a* and copepods were found. Ciliates and *Ceratium* spp. were tested as one group because of the low count of replicates within water-column layers and because they are assumed to have similar swimming abilities. The variability of ciliates and *Ceratium* spp. ($P = 0.03$) and nauplii

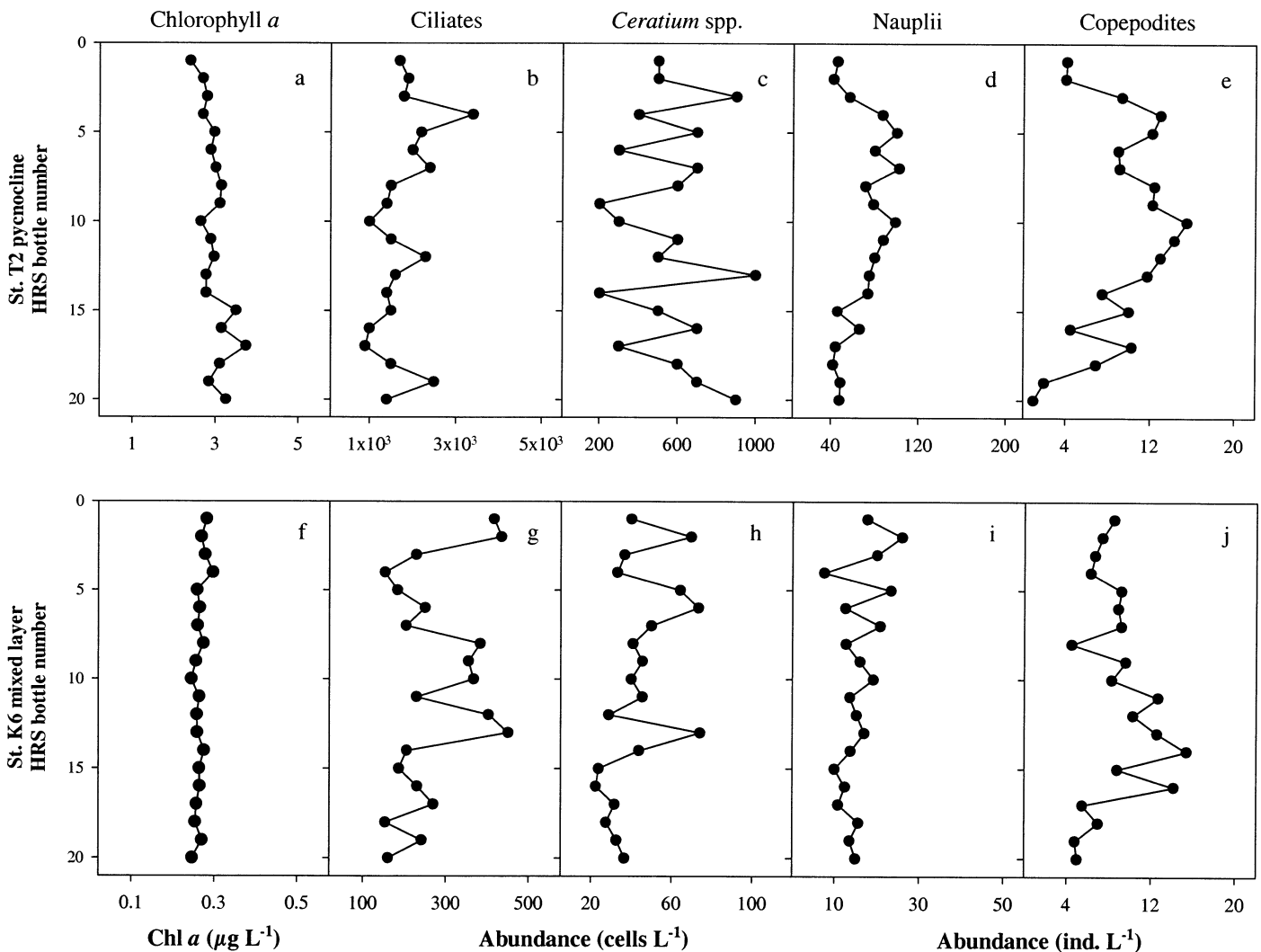


Fig. 6. Microscale variability in distributions of Chl *a*, ciliates, *Ceratium* spp., nauplii, and copepodites in (a–e) the pycnocline at Sta. T2 and (f–j) in the mixed surface layer at Sta. K6. Samples were taken with the HRS equipped with 20 bottles over a 3-m depth stratum.

($P = 0.07$) was significantly lower in the mixed layer compared with the pycnocline and DCM.

The variability of selected organisms was plotted against the turbulent diffusion (Fig. 7). For *Ceratium* spp., ciliates, and nauplii, there was a significant decrease in the CVs with increasing turbulent diffusivity on a log scale. Patchiness was defined according to Owen (1981) as CV values $>33\%$. In our study, turbulent diffusivity values less than 10, 4, and $4 \text{ cm}^2 \text{ s}^{-1}$ allowed a variability of $>33\%$ for *Ceratium* spp., ciliates, and nauplii, respectively. For Chl *a* and copepodites, there was no significant relationship between CVs and turbulent diffusivity.

However, to ensure that the differences in CVs were caused by turbulent diffusivity and not by some other factors, a stepwise multiple regression model with a type I error of 0.05 was applied. The factors considered were turbulent diffusivity, dissipation rate, N^2 , temperature, sample mean, and Chl *a*, all on log scale. For ciliates, *Ceratium* spp., and nauplii, turbulent diffusivity best explained the differences in CVs. For Chl *a* and copepods, no model could be obtained with the considered factors.

Discussion

Microscale patchiness—Turbulent water motions have the potential to influence the distribution patterns of plankton organisms on various scales in the water column. To our knowledge, however, this process has only been assessed through modeling (Jonsson 1989; Davis et al. 1991; Franks 2001) or in field studies over tens of meters (Haury et al. 1990; Visser et al. 2001). In the present study, we were able to study the effect of turbulence on microscale (centimeter to meter) patchiness of different plankton organisms.

The vertical microscale distribution of ciliates, *Ceratium* spp., and nauplii showed a clear response to turbulence. The microscale variability of these organisms decreased dramatically with increasing turbulent diffusion levels. In the study, turbulent diffusion values of less than 10, 4, and $4 \text{ cm}^2 \text{ s}^{-1}$ allowed a variability of $>33\%$ of *Ceratium* spp., ciliates, and nauplii, respectively. In addition, the mean CV was significantly higher in the DCM and pycnocline than at the surface mixed layer, where there was a higher turbulent diffusivity. Owen (1989) also found a greater patchiness at the pycnocline and during low wind conditions, when the turbulent diffusion can be predicted to have been relatively low.

The microzooplankton represents a variety of swimming patterns. Nauplii can swim in straight paths with smooth loops, as observed for *Temora longicornis* (Titelman 2001). Another swimming pattern for nauplii is that of “sink and jump,” which is exhibited by *Acartia tonsa* (Titelman 2001). The protozoan swimming pattern is often characterized as helicoidal paths with a straight axis, and they can also change their swimming direction and magnitude of rotation (Crenshaw 1989). The combination of swimming behavior and chemosensitivity makes it possible for the microzooplankton to locate and exploit food patches (Buskey and Stoecker 1988; Fenchel and Blackburn 1999). The evidence that microzooplankton can influence their vertical position in the water column comes from several studies of diurnal

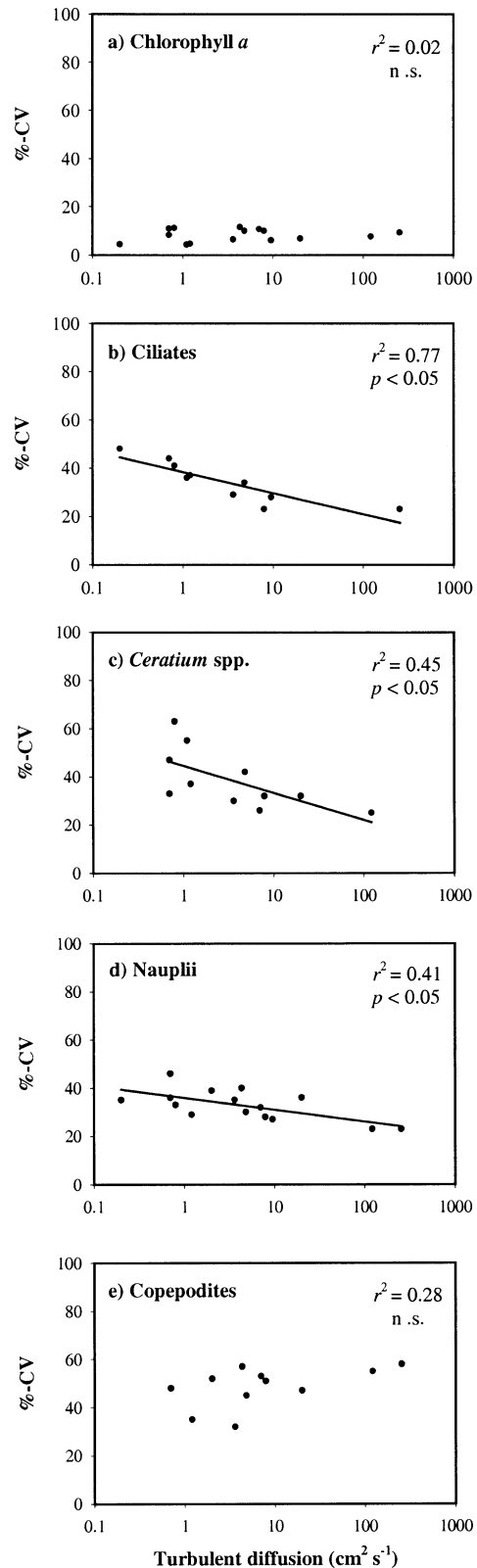


Fig. 7. Regression lines of the CV values in percentage of (a) Chl *a*, (b) ciliates, (c) *Ceratium* spp., (d) nauplii, and (e) copepodites versus the turbulent diffusion on a log scale.

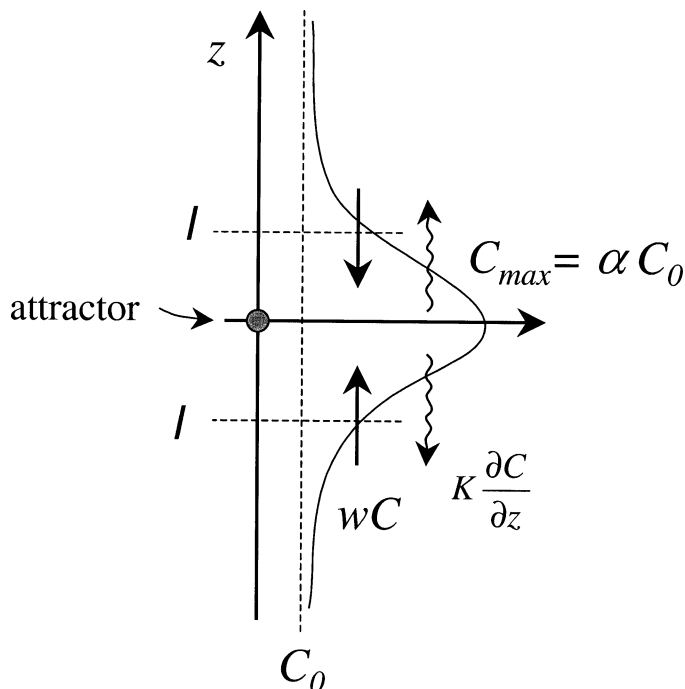


Fig. 8. The diffusion of a swimming organism with a swimming speed w and a concentration C toward an attractor. Steady state is achieved when the diffusive and advective flux are equal. This results in a patch of length scale ℓ , and a maximum concentration of α times the background concentration.

vertical migration (Heaney and Eppley 1981; Olli 1999; Perez et al. 2000) and from other studies of microscale patchiness (Owen 1989; Bjørnsen and Nielsen 1991; Tiselius et al. 1993).

The ability of organisms to form and remain in a patch in a turbulent water column depends on their swimming ability, the turbulent diffusivity, and the nature of the “attractor” (e.g., a patch of food, a chemical, or a specific light intensity) that governs their swimming behavior. If we consider an organism with constant swimming speed w toward an attractor, then the distribution of a patch of such organisms under the influence of diffusion is given by

$$\frac{dC}{dt} = -\frac{\partial F_z}{\partial z} = -\frac{\partial}{\partial z} \left[\pm wC - \kappa \frac{\partial C}{\partial z} \right] \quad (2)$$

where C is the organisms’ concentration and κ is the diffusivity. The \pm indicates the direction change of the organisms’ swimming so that it is toward the attractor (Fig. 8). A patch is maintained in steady state if, at any location, the flux, F_z , is zero. If we define a patch as having a peak concentration $C_{\max} = \alpha C_0$ where C_0 is the background concentration, then the steady-state size of the patch, ℓ , is given by scale analysis as

$$\ell \approx \frac{\alpha - 1}{\alpha + 1} \frac{\kappa}{w} \quad (3)$$

It should be noted that the plankton profile is dynamic, and it is far from certain that concentrations achieve a steady-state distribution. Nonetheless, the steady-state scale ℓ rep-

resents the size to which a patch will converge. If the actual patch size $\ell' < \ell$, diffusion dominates and ℓ' will increase toward ℓ . On the other hand, if $\ell' > \ell$, swimming dominates and ℓ' will decrease toward ℓ . Thus, in the absence of any additional dynamic information, ℓ provides a convenient measure of the expected patch size for a given diffusion rate and swimming ability.

The definition of diffusion in a turbulent water column is not straightforward. It depends on both how particle distributions are measured and their scale. The most common definition is controlled by turbulent eddy diffusivity, K (Eq. 1). This is a property of the flow, and although it can be spatially varying, it is scale independent. Furthermore, it is an Eulerian measure and says something about the probability distribution of particles as they diffuse relative to a fixed point in space.

In comparison, the rate of dispersion following a patch as it moves, a Lagrangian measure, is dependent on the size of the patch. This is because only turbulent eddies smaller than the patch contribute to the relative displacement of particles, whereas larger eddies advect the patch as a whole. This type of dispersion can be formulated as a scale dependent diffusivity, $k(\ell)$, although extreme care must be exercised in applying this. Specifically,

$$k(\ell) = \beta \varepsilon^{1/3} \ell^{4/3} \quad (4)$$

(Richardson 1926; Okubo 1971; Lesieur 1997), where β is a constant (≈ 1) and ε is the turbulent dissipation rate. This formulation is valid for length scales greater than the Kolmogorov scale and less than the integral length scale L . L is a measure of the largest energy containing eddies and defines the upper limit of the inertial subrange of the turbulent energy spectrum. The Kolmogorov scale, η , the lower limit of the inertial subrange, is given by $\eta = (\nu^3/\varepsilon)^{1/4}$, where ν is the kinematic molecular viscosity (Tennekes and Lumley 1972). Similarly, the integral length scale can be estimated by $L = (\nu_T^3/\varepsilon)^{1/4}$, where ν_T is the turbulent eddy viscosity, and the root-mean-square turbulent velocity scale, U , is given by $U = (\nu_T \varepsilon)^{1/4}$ (Mathieu and Scott 2000). For measurements reported herein, L ranges from several meters in the surface mixed layer to several centimeters in the pycnocline. When the patch scale approaches the integral length scale— $\ell \rightarrow L$ —the dispersion coefficient approaches the turbulent eddy diffusivity $k(\ell) \rightarrow K$.

This dual nature of particle dispersion in a turbulent flow has important consequences for how organisms can form and maintain patches. If the attractor is at a fixed position in the water column (a specific light intensity for instance), then the appropriate dispersion coefficient is the turbulent diffusivity (Eq. 1). Setting $\kappa = K$ in Eq. 3 gives

$$\ell_E \approx \frac{\alpha - 1}{\alpha + 1} \frac{e}{N^2 w} \quad (5)$$

That is, as swimming ability decreases or turbulence increases, the patch becomes larger (ℓ_E increases). If, on the other hand, the attractor is a passive tracer (a drifting nutrient or food patch) or is related to the animals own vertical distribution (a swarming-like behavior), then dispersion is scale dependent (Eq. 4), and, setting $\kappa = k(\ell)$ in Eq. 3, the patch size is given by

Table 5. Swimming speed (w) required for organisms to remain in a patch of given size (ℓ_E and ℓ_L) under typical turbulent conditions in the surface mixed layer, the pycnocline, and the deep Chl a maximum (DCM). ε is the measured turbulent dissipation rate, K the turbulent diffusion, N the Brunt-Väisälä frequency, U the rms turbulent velocity, and L the integral length scale.

Layer	ε ($\text{cm}^{-2} \text{s}^{-3}$)	K ($\text{cm}^2 \text{s}^{-1}$)	N (s^{-1})	U (cm s^{-1})	L (cm)	ℓ_E		ℓ_L	
						15	100	15	100
						(cm)	(cm)	(cm)	(cm)
Mixed	0.0021	68	0.005	0.6	120	1.5	0.23	0.1	0.2
Pycnocline	0.0082	2.1	0.026	0.2	5	0.03	0.005	—	—
DCM	0.0006	3.5	0.009	0.3	20	0.08	0.01	0.07	—

$$\ell_L \approx \left(\frac{\alpha + 1}{\alpha - 1} \right)^3 \frac{w^3}{\varepsilon} \quad (6)$$

provided $\ell_L < L$. Curiously, this has the inverse behavior to the above in that as swimming ability decreases or turbulence increases, the patch becomes smaller (ℓ_L increases). For $\ell_L \geq L$, the patch scale $\ell = \ell_E$ as given in Eq. 5. Simply put, the different scaling laws reflect the nature of turbulent mixing in the different regimes. When $\ell < L$, [$\kappa = k(\ell)$], turbulence erodes the edges of a patch without changing its peak concentration significantly. In contrast, when $\ell > L$, ($\kappa = K$), diffusion is of a Fickian nature, broadening the distribution and reducing the peak concentration.

In Table 5 we present representative parameter values for the observations reported herein. The integral length scale ranges from >1 m in the surface mixed layer to 5 cm in the pycnocline. Choosing two representative patch sizes (15 cm, corresponding to the sampling resolution of the HSR, and 1 m) and setting $\alpha = 2$ (corresponding to CV = 33%), we calculate the swimming speed required to maintain the patch for both the Eulerian and Lagrangian cases. In the surface mixed layer, an organism must swim at a speed of 1.5 cm s^{-1} to remain in an Eulerian patch of size 15 cm. In contrast, it must swim only 0.1 cm s^{-1} to remain in a Lagrangian patch of the same dimension. In the pycnocline, where turbulent diffusion is much lower, an organism must swim at only 0.03 cm s^{-1} to remain in a 15-cm patch or 0.005 cm s^{-1} to remain in a 1-m patch. Note that, in the pycnocline, the integral length scale is smaller than the sampling resolution of the HSR so that the Eulerian and Lagrangian patch size estimates are the same. Reported swimming speeds (in the absence of predators) range between 0.02 and 0.06 cm s^{-1} for *Ceratium* spp. (Heaney and Eppley 1981), 0.02 and 0.10 cm s^{-1} for ciliates (Jonsson 1989), and 0.02 and 0.30 cm s^{-1} for nauplii (Mauchline 1998). The calculated swimming velocities necessary to create the observed patchiness in our study are, thus, realistic.

In the previous part of the discussion, the effect of increasing turbulent dissipation rate in counteracting directed plankton swimming through random dispersal through an added turbulent diffusivity was considered. This is, however, not the only possible effect.

Below the Kolmogorov scale, turbulent velocity fluctuations are manifested as laminar shear. The laminar shear field

has a finite vorticity that will cause a solid object to rotate. This induced rotation is hypothesized to interfere with directed swimming. An organism can counteract the torque on its body by either active locomotory compensation or passive reorientation caused—for example, by asymmetry in the density distribution (e.g., Kessler 1986). Vorticity, V , is equal to the shear rate which in turbulent flow below the Kolmogorov scale can be estimated to be of the order (Karp-Boss et al. 1996) of

$$shear = \left(\frac{\varepsilon}{\nu} \right)^{0.5} \quad (7)$$

where ν is the kinematic viscosity ($\sim 0.01 \text{ cm}^2 \text{ s}^{-1}$). The rotation rate of a symmetric solid body is simply half the vorticity (in rad s^{-1}). According to Fenchel (2001), a *Ceratium* cell actively turns at $\sim 0.5 \text{ rad s}^{-1}$. If we set this rotation rate equal to $V/2$, the equation above gives a critical dissipation rate of $\sim 0.01 \text{ cm}^2 \text{ s}^{-3}$. This indicates that dissipation rates in this range may make oriented responses impossible. A further example is ciliates that have been suggested to reorient passively through density asymmetries (Jonsson 1989). Here, ciliates passively reorient at $\sim 0.5 \text{ rad s}^{-1}$ —that is, the critical dissipation rate is approximately similar to the case above. In the present study, however, such a high dissipation rate was only measured at Sta. T2 in the pycnocline (Table 1), so this effect will probably not influence our results.

Copepodite distributions exhibited the highest mean variability of the groups examined (Table 4), and this variability was not correlated to turbulent diffusion or water-column layer. Copepodites are stronger swimmers than microzooplankton, and it is therefore not surprising that they were able to create a higher degree of patchiness than the microzooplankton. Copepodites can detect micropatches of food by chemo- or mechanoreception (Buskey 1984; Tiselius 1992). When a food patch is detected, they can change their motility behavior, approach the patch, and exploit it efficiently (Saiz et al. 1993; Leising and Franks 2000). Using the above models, a copepodite swimming 1 cm s^{-1} would be able to create patchiness (CV $> 33\%$, $\alpha > 2$) on a 1-m scale at turbulent diffusion values $< 300 \text{ cm}^2 \text{ s}^{-1}$ and/or at turbulent dissipation rates $< 0.01 \text{ cm}^3 \text{ s}^{-2}$. The swimming ability of copepodites can also be compared with turbulent

velocities directly. Table 5 shows these to range from 0.6 cm s⁻¹ in the mixed layer to 0.2 cm s⁻¹ in the pycnocline. Thus, copepodites with a swimming velocity ~1 cm s⁻¹ or more will be able to overcome the turbulent mixing. Microscale patchiness of copepodites has also been observed in some earlier field studies (Owen 1989; Tiselius et al. 1994).

On a larger scale, Franks (2001) modeled that copepods swimming >0.1 cm s⁻¹ would leave a 20-m thick mixed layer in ~0.5 h at a maximum turbulent diffusion of 100 cm² s⁻¹. In comparison, it would take 20–25 h for nauplii swimming 0.02–0.03 cm s⁻¹ to exit the surface layer at a turbulent diffusion <10 cm² s⁻¹ (Franks 2001). In the field, Haury et al. (1990) reported that *Oithona* spp. and larveceans vertically separated in the water column during calm conditions with dissipation rates similar to our study. However, during a storm, the dissipation rate increased to 1–10 cm² s⁻³, and the two mesozooplankton groups were redistributed in the water column (Haury et al. 1990). Thus, both model and field work on the scale of centimeters to tens of meters support our results that copepodites can influence their vertical position in the water column at the turbulence levels.

In the present study, however, copepodites could only take advantage of microscale food patches at turbulent diffusion values <4–10 cm² s⁻¹. Above these values, patches of potential prey are dispersed and copepodite growth is reduced (Davis et al. 1991). However, turbulence also increases the encounter rate between predator and prey, and, hence, the feeding rate (Rothschild and Osborn 1988). A dome-shaped relation between ambush feeding rate and turbulence has been observed for example for *A. tonsa* (Saiz and Kiørboe 1995). In the present study, the measured turbulent dissipation rates (<0.04 cm² s⁻³) fell within the positive side of this dome-shaped relation and could thus have been beneficial for copepod feeding and growth. Thus, more studies are needed before the effects of microscale turbulence on copepodite feeding are completely understood.

Microscale patchiness of Chl *a* was not observed in our study, as evidenced by the fact that the CV values were well below the 33% assumed to represent patchiness (Owen 1981). There was no difference in the variability of Chl *a* distributions between water column layers and no relation of this variability to turbulent diffusion. There are several explanations for this homogeneity. First, Chl *a* measurements are averages representing the sum of several types of pigmented plankton cells with different sizes, motility, and physiology. The variability of one species could be counteracted by the variability of other species and the overall patchiness would consequently be more smooth (Owen 1989). In addition, a large proportion of the phytoplankton cells were immobile picoplankton in the Aegean and diatoms in the Skagerrak. These presumably are more easily dispersed by turbulence than mobile forms (Owen 1989; Olli 1999). Finally, the HRS was always deployed within chlorophyll layers, so that chlorophyll gradients were not as steep as observed, for example, by Bjørnsen and Nielsen (1991).

Water-column distributions of plankton organisms—During the summer period (April–September), all stations were stratified, with a DCM. This is a common feature both in

the Skagerrak (Pingree et al. 1982; Kiørboe et al. 1990) and the northern Aegean (Stergiou et al. 1997). However, the DCM did not support a higher abundance of nauplii and copepodites, as has been observed in the North Atlantic, for example (Ortner et al. 1980; Richardson et al. 1998).

The phytoplankton composition in the Skagerrak was mainly chain-forming diatoms, and nutrient levels in the DCM resembled a spring bloom (Maar et al. 2002). Analysis of water masses during the cruise revealed that the DCM at Sta. T2 was associated with a cold low-salinity water patch, which probably was an intrusion of bottom water from the North Sea. Heterotrophic dinoflagellates, including *G. spirale*, that potentially exploit diatoms also had a higher abundance in the DCM. The abundance of nauplii and copepodites, on the other hand, was lower here than at the pycnocline. The two most abundant copepods were *Paracalanus* and *Oithona* spp. They probably graze the protozooplankton and smaller phytoplankton cells, which had a biomass of 48 µg C L⁻¹ at the DCM and 19 µg C L⁻¹ at the pycnocline. However, average food availability was below the 200 µg C L⁻¹, which should be growth limiting for *Oithona* spp. (Kiørboe and Sabatini 1995).

By way of contrasts, the DCM in the northern Aegean consisted of picoplankton that are not a suitable food source for nauplii and copepodites (Calbet et al. 2000). In the frontal area, ciliates, dinoflagellates, and small diatoms had the highest abundance in the surface layer and are an important food source for nauplii and copepodites. Despite the low Chl *a* concentrations, the highest abundance of nauplii and copepodites was, therefore, found in the mixed and pycnocline layer. Outside the frontal area, the water column was stratified by a thermocline. Here, there was no obvious depth partitioning of zooplankton. Generally, the average biomass of phytoplankton and protozooplankton suitable for copepodite was very low in the northern Aegean, and, presumably, food was limiting for copepodite growth. Microscale food patchiness would, therefore, be important for copepodite growth and survival in both areas during the stratified summer period.

Intuitively, we expect the ability of plankton organisms to distribute themselves patchily in the environment to be greatest under low turbulence conditions. We also expect the strongest swimmers to have the greatest potential to control their position in the water column. So far, however, it has not been possible to confirm these predictions with field data. Herein we present simultaneous measurements of microscale patchiness of zooplankton organisms and microscale turbulence. We have documented that the variability in distributions of microzooplankton (ciliates, *Ceratium* spp., and nauplii) decreased dramatically with increasing turbulent mixing. For these organisms, microscale patches could only persist at turbulent diffusion values <4–10 cm² s⁻¹. For Chl *a*, no microscale variability in distributions was observed. This may have been due to the presence of nonmotile phytoplankton at the time of the study. However, it is also possible that the variability of different species was masked by the fact that chlorophyll measurements represent average distributions of phytoplankton. Copepodites with the highest swimming potential, on the other hand, exhibited the highest microscale patchiness, and this patchiness was independent

of turbulence. In conclusion, the present study demonstrates that a range of planktonic organisms have the abilities and behavioral adaptations that allow them to form and remain within vertical patches of higher food concentrations, thereby increasing their overall survival success.

References

- ANDERSEN, V., A. GUBANOVA, P. NIVAL, AND T. RUELLET. 2001. Zooplankton community during the transition from spring bloom to oligotrophy in the open NW Mediterranean and effects of wind events. 2. Vertical distributions and migrations. *J. Plankton Res.* **23**: 243–261.
- BJØRNSEN, P. K., AND T. G. NIELSEN. 1991. Decimeter scale heterogeneity in the plankton during a pycnocline bloom of *Gyrodinium aureolum*. *Mar. Ecol. Prog. Ser.* **73**: 263–267.
- BUSKEY, E. J. 1984. Swimming patterns as an indicator of the roles of copepod sensory systems in the recognition of food. *Mar. Biol.* **79**: 165–175.
- , AND D. K. STOECKER. 1988. Locomotory patterns of the planktonic ciliate *Favella* sp.—adaptations for remaining within food patches. *Bull. Mar. Sci.* **43**: 783–796.
- CALBET, A., M. R. LANDRY, AND R. D. STEINBERG. 2000. Copepod grazing in a subtropical bay: Species-specific responses to a midsummer increase in nanoplankton standing stock. *Mar. Ecol. Prog. Ser.* **193**: 75–84.
- CRENSHAW, H. C. 1989. Kinematics of helical motion of microorganisms capable of motion with four degrees of freedom. *Biophys. J.* **56**: 1029–1035.
- DAVIES, R. E. 1996. Sampling turbulent dissipation. *J. Phys. Oceanogr.* **26**: 341–358.
- DAVIS, C. S., G. R. FLIERL, P. H. WIEBE, AND P. S. FRANKS. 1991. Micropatchiness, turbulence and recruitment in plankton. *J. Mar. Res.* **49**: 109–151.
- FENCHEL, T. 2001. How dinoflagellates swim. *Protist* **152**: 329–338.
- , AND N. BLACKBURN. 1999. Motile chemosensory behaviour of phagotrophic protists: Mechanisms for and efficiency in congregating at food patches. *Protist* **150**: 325–336.
- FRANKS, P. S. 2001. Turbulence avoidance: An alternate explanation of turbulence-enhanced ingestion rates in the field. *Limnol. Oceanogr.* **46**: 959–963.
- HAURY, L. R., H. YAMAZAKI, AND E. C. ITSWEIRE. 1990. Effects of turbulent shear-flow on zooplankton distribution. *Deep-Sea Res.* **37**: 447–461.
- HEANEY, S. I., AND R. W. EPPLEY. 1981. Light, temperature and nitrogen as interacting factors affecting diel vertical migrations of dinoflagellates in culture. *J. Plankton Res.* **3**: 331–344.
- JONSSON, P. R. 1989. Vertical-distribution of planktonic ciliates—an experimental analysis of swimming behavior. *Mar. Ecol. Prog. Ser.* **52**: 39–53.
- KARP-BOSS, L., E. BOSS, AND P. A. JUMARS. 1996. Nutrient fluxes to planktonic osmotrophs in the presence of fluid motion. *Oceanogr. Mar. Biol.* **34**: 71–107.
- KESSLER, J. O. 1986. The external dynamics of swimming microorganisms. *Prog. Phycol. Res.* **4**: 257–307.
- KIØRBOE, T., H. KAAS, B. KRUSE, F. MØHLENBERG, P. T. TISELIUS, AND G. ÆRTEBJERG. 1990. The structure of the pelagic food web in relation to water column structure in the Skagerrak. *Mar. Ecol. Prog. Ser.* **59**: 19–32.
- , AND T. G. NIELSEN. 1994. Regulation of zooplankton biomass and production in a temperate, coastal ecosystem: 1. Copepods. *Limnol. Oceanogr.* **39**: 493–507.
- , AND M. SABATINI. 1995. Scaling of fecundity, growth and development in marine planktonic copepods. *Mar. Ecol. Prog. Ser.* **120**: 285–298.
- LEISING, A. W., AND P. S. FRANKS. 2000. Copepod vertical distribution within a spatially variable food source: A simple foraging-strategy model. *J. Plankton Res.* **22**: 999–1024.
- LESIEUR, M. 1997. Turbulence in fluids. Kluwer.
- MAAR, M., T. G. NIELSEN, K. RICHARDSON, U. CHRISTAKI, O. S. HANSEN, T. ZERVOUDAKI, AND E. D. CHRISTOU. 2002. Spatial and temporal variability of the food web structure during the spring bloom in the Skagerrak. *Mar. Ecol. Prog. Ser.* **239**: 11–29.
- MACKAS, D. L., H. SEFTON, C. B. MILLER, AND A. RAICH. 1993. Vertical habitat partitioning by large calanoid copepods in the oceanic sub-arctic Pacific during spring. *Prog. Oceanogr.* **32**: 259–294.
- MATHIEU, J., AND J. SCOTT. 2000. An introduction to turbulent flow. Cambridge Univ. Press.
- MAUHLIN, J. 1998. The biology of calanoid copepods. *Adv. Mar. Biol.* **33**: 1–710.
- MENDEN-DEUER, S., AND E. J. LESSARD. 2000. Carbon to volume relationships for dinoflagellates, diatoms, and other protist plankton. *Limnol. Oceanogr.* **45**: 569–579.
- MOUM, J. N., M. C. GREGG, R. C. LIEN, AND M. E. CARR. 1995. Comparison of turbulence kinetic energy dissipation estimates from two ocean microstructure profilers. *J. Atmos. Oceanic Technol.* **12**: 346–366.
- , AND R. G. LUECK. 1985. Causes and implications of noise in oceanic dissipation measurements. *Deep-Sea Res.* **32**: 379–390.
- NIELSEN, T. G., AND P. J. HANSEN. 1999. Dyreplankton i danske farvande (in Danish). Tema-rapport fra DMU, Miljø- og Energinisteriet.
- OAKEY, N. S. 1982. Determination of the rate of dissipation turbulent energy from simultaneous temperature and velocity shear microstructure measurements. *J. Phys. Oceanogr.* **12**: 256–271.
- OKUBO, A. 1971. Oceanic diffusion diagrams. *Deep-Sea Res.* **18**: 789–802.
- OLLI, K. 1999. Diel vertical migration of phytoplankton and heterotrophic flagellates in the Gulf of Riga. *J. Mar. Syst.* **23**: 145–163.
- ORTNER, P. B., P. H. WIEBE, AND J. L. COX. 1980. Relationships between oceanic epizooplankton distributions and the seasonal deep chlorophyll maximum in the northwestern Atlantic Ocean. *J. Mar. Res.* **38**: 507–531.
- OSBORN, T. R. 1980. Estimates of the local rate of vertical diffusion from dissipation measurements. *J. Phys. Oceanogr.* **10**: 83–89.
- OWEN, R. W. 1981. Microscale plankton patchiness in the larval anchovy environment. *Rapp. P.-v. Réun. Cons. Int. Explor. Mer.* **178**: 364–368.
- . 1989. Microscale and finescale variations of small plankton in coastal and pelagic environments. *J. Mar. Res.* **47**: 197–240.
- PEREZ, M. T., J. R. DOLAN, F. VIDUSSI, AND E. FUKAI. 2000. Diel vertical distribution of planktonic ciliates within the surface layer of the NW Mediterranean (May 1995). *Deep-Sea Res.* **47**: 479–503.
- PETERS, H., M. C. GREGG, AND J. M. TOOLE. 1988. On the parameterization of equatorial turbulence. *J. Geophys. Res.* **93**: 1199–1218.
- PINGREE, R. D., P. M. HOLLIGAN, G. T. MARDELL, AND R. P. HARRIS. 1982. Vertical distribution of plankton in the Skagerrak in relation to doming of the seasonal thermocline. *Cont. Shelf Res.* **1**: 209–219.
- PRANDKE, H., K. HOLTSCH, AND A. STIPS. 2000. MITEC technology development: The microstructure/turbulence measuring system MSS: Technical report EUR 19733 EN. European Commission.
- , AND A. STIPS. 1998. Test measurements with an operational

- microstructure-turbulence profiler: Detection limit of dissipation rates. *Aquat. Sci.* **60**: 191–209.
- RICHARDSON, K., T. G. NIELSEN, F. B. PEDERSEN, J. P. HEILMANN, B. LØKKEGAARD, AND H. KAAS. 1998. Spatial heterogeneity in the structure of the planktonic food web in the North Sea. *Mar. Ecol. Prog. Ser.* **168**: 197–211.
- RICHARDSON, L. F. 1926. Atmospheric diffusion shown on a distance-neighbor graph. *Proc. R. Soc. Lond. A* **110**: 709–737.
- ROHDE, J. 1998. The Baltic and North Seas: A process-oriented review of the physical oceanography. Coastal segment, p. 699–732. *In* A. R. Robinson and K. H. Brink [eds.], *The sea*. V. 11. Wiley.
- ROTHSCHILD, B. J., AND T. R. OSBORN. 1988. Small-scale turbulence and plankton contact rates. *J. Plankton Res.* **10**: 465–474.
- SAIZ, E., AND T. KIØRBOE. 1995. Predatory and suspension-feeding of the copepod *Acartia tonsa* in turbulent environments. *Mar. Ecol. Prog. Ser.* **122**: 147–158.
- , P. TISELIUS, P. R. JONSSON, P. G. VERITY, AND G.-A. PAFENHÖFER. 1993. Experimental records of the effects of food patchiness and predation on egg production of *Acartia tonsa*. *Limnol. Oceanogr.* **38**: 280–289.
- STERGIOU, K. I., E. D. CHRISTOU, D. GEORGIOPOULOS, A. ZENETOS, AND C. SOUVERMEZOGLOU. 1997. The Hellenic seas: Physics, chemistry, biology and fisheries. *Oceanogr. Mar. Biol.* **35**: 415–538.
- STIPS, A., H. PRANDKE, AND U. TSCHESCHE. 2001. Report on processing of microstructure data from the KEYCOP-8/2000 campaign: Technical report I.01.57. European Commission.
- TENNEKES, H., AND J. L. LUMLEY. 1972. *A first course of turbulence*. MIT Press.
- TISELIUS, P. 1992. Behavior of *Acartia tonsa* in patchy food environments. *Limnol. Oceanogr.* **37**: 1640–1651.
- , P. R. JONSSON, AND P. G. VERITY. 1993. A model evaluation of the impact of food patchiness on foraging strategy and predation risk in zooplankton. *Bull. Mar. Sci.* **53**: 247–264.
- , G. NIELSEN, AND T. G. NIELSEN. 1994. Microscale patchiness of plankton within a sharp pycnocline. *J. Plankton Res.* **16**: 543–554.
- TITELMAN, J. 2001. Swimming and escape behavior of copepod nauplii: Implications for predator-prey interactions among copepods. *Mar. Ecol. Prog. Ser.* **213**: 203–213.
- VISSER, A. W., H. SAITO, E. SAIZ, AND T. KIØRBOE. 2001. Observations of copepod feeding and vertical distribution under natural turbulent conditions in the North Sea. *Mar. Biol.* **138**: 1011–1019.
- YENTSCH, C. S., AND D. W. MENZEL. 1963. A method for the determination of phytoplankton chlorophyll and phaeophytin by fluorescence. *Deep-Sea Res.* **10**: 221–231.

Received: 29 July 2002

Accepted: 10 December 2002

Amended: 8 January 2003